Operations Research Perspectives 8 (2021) 100207

Contents lists available at ScienceDirect

Operations Research Perspectives

journal homepage: www.elsevier.com/locate/orp

Evolutionary optimized Padé approximation scheme for analysis of covid-19 model with crowding effect

Javaid Ali [a], Ali Raza [b,c], Nauman Ahmed [d], Ali Ahmadian [e,f,h,*], Muhammad Rafiq [g], Massimiliano Ferrara [h]

[a] Department of Mathematics, GGCT, Punjab Higher Education Department, Lahore, Pakistan
[b] Department of Mathematics, National College of Business Administration and Economics Lahore, Pakistan
[c] Department of Mathematics, Govt. Maulana Zafar Ali Khan Graduate College Wazirabad, Punjab Higher Education Department, Lahore, Pakistan
[d] Department of Mathematics and Statistics, The University of Lahore, Pakistan
[e] Institute of IR 4.0, The National University of Malaysia, 43600 UKM, Selangor, Malaysia
[f] Department of Mathematics, Near East University, Nicosia, TRNC, Turkey
[g] Department of Mathematics, Faculty of Sciences, University of Central Punjab, Lahore, Pakistan
[h] Department of Law, Economics and Human Sciences & Decisions Lab, University Mediterranea of Reggio Calabria, 89125, Reggio Calabria Italy

ARTICLE INFO

Keywords:
Evolutionary computing
Padé approximation
Covid-19 model
Crowding effect
Hybrid optimizer

ABSTRACT

This work presents a novel evolutionary computation-based Padé approximation (EPA) scheme for constructing a closed-form approximate solution of a nonlinear dynamical model of Covid-19 disease with a crowding effect that is a growing trend in epidemiological modeling. In the proposed framework of the EPA scheme, the crowding effect-driven system is transformed to an equivalent nonlinear global optimization problem by assimilating Padé rational functions. The initial conditions, boundedness, and positivity of the solution are dealt with as problem constraints. Keeping in view the complexity of formulated optimization problem, a hybrid of differential evolution (DE) and a convergent variant of the Nelder-Mead Simplex algorithm is also proposed to obtain a reliable, optimal solution. The comparison of the EPA scheme results reveals that optimization results of all formulated optimization problems for the Covid-19 model with crowding effect are better than those of several modern metaheuristics. EPA-based solutions of the Covid-19 model with crowding effect are in good agreement with those of a well-practiced nonstandard finite difference (NSFD) scheme. The proposed EPA scheme is less sensitive to step lengths and converges to true equilibrium points unconditionally.

1. Literature survey

Bats were the source of Covid-19, which SARS-nCoV2 caused. SARS-CoV1 and MERS-CoV1 are similar viruses. Its genetic material, RNA, is encased in a lipid-layered surface with spike proteins that resemble the shape of a crown, hence the name corona. In December 2019, it was first seen in Wuhan, China. In February 2020, China, Italy, Iran, and South Korea were present. Then, by the middle of March 2020, it had spread all over the planet. Since then, it has appeared in waves in different parts of the world due to significantly modified forms. The elderly, immune-compromised, diabetics, cancer patients, and heart patients are the most vulnerable. It takes 4–14 days to incubate. The majorities of cases are mild, with symptoms such as fever, illness, and cough. A cytokine storm can induce shortness of breath, body aches, nausea, pneumonia, respiratory failure, and death in severe circumstances. It spreads through the inhalation of deadly virus respiratory droplets produced by infected people and breathed by adjacent people. To detect suspected patients, we employ PCR tests, and to see suspected recovered patients; we use antibody tests. Distancing, masking, hand washing, lockdown, and mass vaccination are still being used to manage the disease. Since its inception, vaccination has shown promising effects. Nonetheless, it is proving to be the only reliable way out of the problem.

Daniel Bernoulli developed the first mathematical epidemic model in 1760 to assess the efficacy of the smallpox vaccine. Modeling nowadays incorporates continual advancements in computational tools and illness data. Understanding disease dynamics, evaluating viable control techniques, and predicting future outbreaks are all aided by this information. They help to flatten the curve of the Covid-19 pandemic in the country

* Corresponding author.
E-mail address: aseyedal@kean.edu (A. Ahmadian).

https://doi.org/10.1016/j.orp.2021.100207
Received 29 June 2021; Received in revised form 1 November 2021; Accepted 8 November 2021
Available online 24 November 2021

by predicting disease patterns. The mathematical modeling of biological processes allows epidemiological assumptions to be revised. As a result, we can put our grasp of disease epidemiology to the test by comparing model findings to observed trends.

In 2020, Zeb et al. proposed a SEIQR mathematical model to control Covid-19 propagation via optimal control techniques [1]. Recently, in 2021, several complex epidemiological models have been submitted. For example, Riyapan et al. presented a SEIIQRD mathematical model of Covid-19 in Bangkok, which explains the dynamical analysis of the proposed model [2]. Oud et al. suggested a SEIAQHRM mathematical model for Covid-19 to study the quarantine effect, which describes how curable the vaccination for the dreadful virus or which strategy may be adopted during the vaccination [3]. Shaikh et al. presented a SEIARQ model of the coronavirus disease to check its outbreak in India to explain the strain of the virus through mathematical modeling [4]. Ahmed et al. presented a SEQIR model of coronavirus to study the relationship between symptomatic and asymptomatic classes [5]. In 2020, Ullah et al. introduced a SEIIQIIR model to comprehend the use of different drugs as vaccinations [6]. Peter et al. (in 2021) presented a SEIQR model to estimate the damages caused by a coronavirus in Pakistan [7]. Recently, Nazir et al. studied a SEIARW model to numerically analyze the effectiveness of the Euler method [8]. Kyrychko et al. presented a SEIARD model to calculate the propagation and role of agents in spreading coronavirus in Ukraine [9]. Khoshnaw suggested that medical awareness and keeping social distances were more effective in controlling the spread of coronaviruses [10]. Sasmita et al. presented a model that considers different subpopulations interactions for control of Covid-19 [11]. In 2020, Tiwar et al. predicted the importance of lockdown for controlling the spread of Covid-19 disease in India through the SEIRD model [12]. Wang et al., in 2021, proposed a SEIRD model which incorporates the different ways for the spread of disease [13]. Baek et al. proposed the SEIR model for controlling the spread of Covid-19 via quarantine and hospitalization [14]. Ardila et al. suggested that isolation and staying away are the key factors preventing the spread of Covid-19 [15]. Peter et al. presented the susceptible (S), Exposed (E), infected (I), Quarantine (Q), carriers (C), and recovered (R) model for controlling the disease in Nigeria [16]. In 2020, Moyles et al. proposed that social distancing is highly effective in preventing the spread of infection [17]. Ko et al. suggested the correlation of SEIR-HCD and SEIR-D model for the control of disease in Moscow [18]. Recently, Harjule has indicated the importance of modeling in controlling the spread of Covid-19 [19]. In 2020, Kim et al. proposed that staying home, keeping distance and early detection are the core points in controlling the spread of Covid-19 [20]. Some well-known models related to Covid-19 with different mathematical strategies are presented in the literature referred to in this study [21–29].

Modeling differential equations as equivalent optimization problems [30–38] is one of the most modern techniques to obtain reliable solutions, especially when the traditional method lacks handling one or more aspects of the physical phenomena. The related examples of such modeling include solving nonlinear ordinary differential equations, inverse partial differential equations, and epidemiological models. Ali et al. [37, 38] proposed a novel evolutionary Padé approximation (EPA) scheme for solving epidemiological models and nonlinear partial differential equations. Padé rational approximation functions are a vital research area due to their tremendous applications in several scientific areas [39, 40]. Henri Eugene Padé [41] established suitable Padé approximations for series expansion of functions even where the Taylor series failed to converge. In past studies, Padé approximations were employed to enhance the precision of the solution only obtained by other master methods based on power series [42], differential transform [43], homotopy analysis [44], and Adomian decomposition [45].

The Padé approximation-based formulated optimization problem from differential equations may involve complex non-convexity, multimodality, and non-differentiability. Traditional mathematical programming approaches are not capable of solving such complex problems. On the other hand, evolutionary algorithms are capable of solving almost all kinds of optimization problems. They belong to a general class of optimization techniques known as metaheuristics. Metaheuristics are designed by imitating some natural procedures like flashing behavior of fireflies [46], student-teacher learning procedure [47], swarming [48], evolution [49, 50], water dynamics [51–53], sport strategies [54], food foraging behavior [55], animals' hunting [56], etc. For more detailed studies, one may consult the survey article by Alexandros and Georgios [57].

Unfortunately, the theoretical authentication of metaheuristics is still deficient. Past studies [46, 58] have highlighted some severe challenges in the applications of metaheuristics. Despite their successful applications to very diverse problems, there are No Free Lunch (NFL) theorems [58] which reveal that one cannot guarantee that a method effective for one set of trials will be equally efficient for the other collection of problems. Keeping the complexity of the underlying problem in view, hybridization is an effective technique to improve the performance of the selected global search optimizer. As far as the present study is concerned, we have chosen a widely used classic version [59] of the worldwide search Differential Evolution (DE) algorithm [49] in combination with a convergent variant [60] of the Nelder-Mead Simplex (NMS) method [61] to obtain better results.

This work presents the first EPA scheme-based formulation and solution of the Covid-19 disease dynamical model with crowding effect as an optimization problem to the best of our knowledge. In the original proposal [37, 38] of the EPA scheme, the focus on optimization was minimal, and the underlying model was comparatively less complex. But the present study adds some new aspects to the theory of the EPA scheme for solving epidemiological models with crowding effect. The architecture of the EPA scheme consists of the following novel features that were lacking in the previous studies.

(i) The impact of variation in the order of Padé approximants for state variables on resulting cost function has been studied.
(ii) A comparative study of the performance of several modern metaheuristics on formulated equivalent unconstrained optimization problems has been conducted, and the essence of the proposed hybrid evolutionary optimizer has been elaborated.
(iii) The strength of mathematical programming and metaheuristics for solving complex epidemiological models has been highlighted.
(iv) The EPA scheme preserves all vital properties like positivity, boundedness, feasibility, convergence to equilibrium points, etc., by enforcing the solution to satisfy related problem constraints.
(v) The EPA scheme's convergence speed is high compared to a well-practiced NonstandardNonstandard Finite Difference (NSFD) [62] structure-preserving method.

The remainder of the manuscript is organized as follows: Section 2 presents the formulation of the Covid-19 model with crowing effect along with stability analysis of equilibrium points. Section 3 consists of a detailed procedure of all components of the EPA scheme for solving the Covid-19 model with the crowing effect. Section 4 presents a rigorous analysis of the results of the EPA scheme in many aspects of reliability, efficiency, and structure-preserving ability. The concluding remarks are also presented in the end.

2. Model formulation

With the help of the theory of population dynamics, we consider the whole population is denoted by N, and subpopulations are defined as Susceptible humans $S(t)$, Infected humans $I(t)$, and Recovered humans $R(t)$. Furthermore, the fixed values of the model are defined as: μ : (recruitment rate /mortality rate of humans), β : (the force of infection), $\frac{1}{1+\alpha I}$:(represents the crowding effect in a population), and γ : (the

rate of recovery due to immunity or vaccination). The dreadful situation will occur when the "α" increases continuously. Eventually, the rate of active cases is elevated. Hence, there is a direct relationship between the crowding factor and active patients of coronavirus. Here arises the inevitability of controlling the parameter α so that the dynamics of coronavirus disease may be governed. From the mathematical modeling point of view, we achieve the following coupled nonlinear dynamical system:

$$\frac{dS}{dt} = \mu N - \frac{\beta SI}{1+\alpha I} - \mu S \tag{1}$$

$$\frac{dI}{dt} = \frac{\beta SI}{1+\alpha I} - -(\gamma+\mu)I \tag{2}$$

$$\frac{dR}{dt} = \gamma I - - \mu R \tag{3}$$

2.1. Analysis of model

2.1.1. Positivity and boundedness

The feasible region of the system (1–3) as follows:

$$H = \left\{(S,I,R)\epsilon\mathbb{R}^3_+ : \mathrm{S}+\mathrm{I}+\mathrm{R} = N,\ S \geq 0, \mathrm{I}\ \geq 0, R \geq 0\right\}$$

For this purpose, we will investigate the following results.

Theorem 1. *The solutions $(S,I,R)\epsilon\mathbb{R}^3_+$ of the system (1–3) are positive at any time $t \geq 0$, with given non-negative initial conditions.*

Proof: It is clear from the system (1–3) as follows:

$$\frac{dS}{dt}|_{S=0} = \mu N \geq 0,\ \frac{dI}{\mathrm{dt}}|_{I=0} = 0 \geq 0,\ \frac{dR}{\mathrm{dt}}|_{R=0} = \gamma I \geq 0.$$

Theorem 2. *The solutions $(S,I,R)\epsilon\mathbb{R}^3_+$ of the system (1–3) are bounded.*

Proof: Let us consider the population function as follows:

$$N(\mathrm{t}) = S + \mathrm{I} + \mathrm{R}$$

$$\frac{dN}{dt} = \frac{dS}{dt} + \frac{dI}{dt} + \frac{dR}{dt}$$

$$\frac{dN}{dt} = \mu N - \mu(S+I+R),\ S+I+R = N$$

$$\frac{dN}{dt} = \mu N - \mu N$$

$$\frac{dN}{dt} = 0.$$

Since the total population is fixed, the system's solution (1–3) is bounded and lies in the feasible region H.

2.1.2. Model equilibria

The system (1–3) admits two types of equilibria as follows:

Disease free equilibrium (DFE) $E_0 = (N,0,0)$.

Endemic equilibrium (EE) $E_* = (S_*, I_*, R_*)$.

$$S^* = a_1 + a_2 I_*\ I_* = \frac{-A_2 + \sqrt{A_2^2 - 4A_1A_3}}{2A_1},\ R^* = \frac{\gamma I_*}{\mu},$$

where, $a_1 = \frac{(\gamma+\mu)}{\beta}$, $a_2 = \frac{\alpha(\gamma+\mu)}{\beta}$, $A_2 = +(\beta a_1 + \mu(a_1+a_2)\alpha - \mu N\alpha)$, $A_1 = a_2(\beta+\alpha)$, $A_3 = (\mu a_1 - - \mu N)$.

Note that, the reproduction number of the model $\mathscr{R}_0 = \rho(\mathrm{F}V^{-1}) = \frac{\beta N}{\gamma+\mu}$.

2.2. Local stability analysis of the model

Theorem 3. *The system (1–3) is locally stable related to the virus-free equilibrium point E_0, if $\mathscr{R}_0 < 1$ and unstable if $\mathscr{R}_0 > 1$.*

Proof: For local stability, the Jacobian of the system (1–3) is as follows:

$$j = \begin{pmatrix} -\mu - \frac{\beta SI}{1+\alpha I} & -\frac{\beta S}{(1+\alpha I)^2} & 0 \\ \frac{\beta SI}{1+\alpha I} & \frac{\beta S}{(1+\alpha I)^2} - (\mu+\gamma) & 0 \\ 0 & \gamma & -\mu \end{pmatrix}.$$

At E_0, *the Jacobian becomes*

$$j(E_0) = \begin{pmatrix} -\mu & -\beta N & 0 \\ 0 & \beta N - (\gamma+\mu) & 0 \\ 0 & \gamma & -\mu \end{pmatrix}.$$

These are the following eigen values as

$$\lambda_1 = -\mu < 0,\ \lambda_2 = \beta N - (\gamma+\mu) < 0,\ \text{if } \mathscr{R}_0 < 1,\ \text{if } \lambda_3 = -\mu < 0.$$

Thus, point E_0 is locally asymptotically stable.

Theorem 4. *For $\mathscr{R}_0 > 1$, the system (1–3) at the positive endemic equilibrium E_* of the system (1–3) is locally stable.*

Proof: The Jacobean matrix of system (1–3) is as follows:

$$j = \begin{pmatrix} -\mu - \frac{\beta I}{1+\alpha I} & -\frac{\beta S}{(1+\alpha I)^2} & 0 \\ \frac{\beta I}{1+\alpha I} & \frac{\beta S}{(1+\alpha I)^2} - (\mu+\gamma) & 0 \\ 0 & \gamma & -\mu \end{pmatrix}.$$

At E_*, *the jacobian becomes*

$$j(E_*) = \begin{pmatrix} -\mu - \frac{\beta I_*}{1+\alpha I_*} & -\frac{\beta S_*}{(1+\alpha I_*)^2} & 0 \\ \frac{\beta I_*}{1+\alpha I_*} & \frac{\beta S_*}{(1+\alpha I_*)^2} - (\mu+\gamma) & 0 \\ 0 & \gamma & -\mu \end{pmatrix}.$$

Which yields one eigenvalue $\lambda = -\mu < 0$ and the characteristics equation

$$\lambda^2 + \left(\mu + \frac{\beta I_*}{1+\alpha I_*} - -\frac{\beta S_*}{(1+\alpha I_*)^2} + (\mu+\gamma)\right)\lambda + \left(\mu + \frac{\beta I_*}{1+\alpha I_*}\right)\left(\frac{\beta S_*}{(1+\alpha I_*)^2} + (\mu+\gamma)\right) + \left(\frac{\beta S_*}{(1+\alpha I_*)^2}\right)\left(\frac{\beta I_*}{1+\alpha I_*}\right) = 0.$$

It is clear, for $\mathscr{R}_0 > 1$, and by using Routh Hurwitz criteria for 2nd order

$$\left(\mu + \frac{\beta I_*}{1+\alpha I_*} - \frac{\beta S_*}{(1+\alpha I_*)^2} + (\mu+\gamma)\right) = (\mu + \frac{\beta I_*}{1+\alpha I_*} - \frac{(\mu+\gamma)}{(1+\alpha I_*)^2} + (\mu+\gamma)) > 0.$$

And

$$\mu + \frac{\beta I_*}{1+\alpha I_*})\left(\frac{\beta S_*}{(1+\alpha I_*)^2} + (\mu+\gamma)\right) + \left(\frac{\beta S_*}{(1+\alpha I_*)^2}\right)\left(\frac{\beta I_*}{1+\alpha I_*}\right) > 0.$$

Hence, the system (1–3) is locally stable at E_* for $\mathscr{R}_0 > 1$. The proof is complete.

3. Evolutionary Padé approximation (EPA) scheme for covid-19 model with crowding effect

This section is dedicated to the architecture of the EPA scheme for solving the approximate model. The first component of the proposed scheme constructs an equivalent optimization problem by modeling the coupled system of governing equations described in Eqs. (1–3) using the Padé approximation. The second component executes the optimization task by implementing a classical DE algorithm [59]. To obtain global optimum solutions of the formulated problem, DE is further hybridized with a non-stagnated Nelder-Mead Simplex (NS-NMS) algorithm [60] that is a convergent variant of a simplex search based Nelder-Mead method [61]. The unconstrained minimization objective function $\psi(\boldsymbol{x})$ is highly nonlinear and may contain discontinuities and several local optima.

Fig. 1.

Moreover, as the orders $(M_v,\ N_v)$ of Padé approximations increase, the curse of dimensionality involves. In the presence of such challenges, the use of an efficient and reliable optimization algorithm is complementary. We use the DE algorithm, which has earned very high ranks in the optimization community due to its tremendous success in almost all optimization problems.

3.1. Formulation of equivalent optimization problem

Formulation of equivalent optimization problem consists of four key factors that are (i) approximating the state variables by Padé approximations (ii) conversion of each governing equation to a residual function (iii) handling the initial conditions as problem constraints (iv) use of penalty functions for obtaining unconstrained global optimization problem. The global optimum solution of the resulting unconstrained optimization problem is analogous to the solution of the Covid-19 model with a crowding effect.

(I) *Approximation by Padé rational functions*

First, we approximate the state variables $S(t)$, $I(t)$, and $R(t)$ by Padé rational functions of appropriate orders. For any $v \in \{S,\ I,\ \mathrm{R}\}$, let $A_v(t)$ and $B_v(t)$ denote polynomial functions of variable t having degrees M_v and N_v, respectively. Then Padé rational approximation functions of orders $(M_v, N_v) \in \mathbb{W}^2$ [37, 38] for state variables are:

$$S(t) \approx p_S(t) = \frac{A_S(t)}{B_S(t)},\ I(t) \approx p_I(t) = \frac{A_I(t)}{B_I(t)},\ R(t) \approx p_R(t) = \frac{A_R(t)}{B_R(t)}.$$

Here $A_v(t)$ and $B_v(t)$ are polynomial functions with real coefficients a_{vj}, b_{vj} for each $j \in \mathbb{W}$ defined by:

$$A_v(t) = \sum_{j=0}^{M_v} a_{vj}t^j;\ B_v(t) = \sum_{j=0}^{N_v} b_{vj}t^j.$$

The derivative of $p_v(t)$ with respect to t can be expressed as under:

$$p'_v(t) = \frac{A'_v(t) - p_v(t)B'_v(t)}{B_v(t)} \forall\ v \in \{S, I, R\}$$

(I) *Formation of residual functions*

The domain of t for the Covid-19 model is $[0, \infty)$. For some positive integer K, let us consider a monotone strictly increasing sequence $\{t_0,\ t_1,\ t_2,\ t_3, \ldots,\ t_K\}$ as a subset of the domain $[0,\ \infty)$. The proposed scheme does not depend on step length to create such a sequence, but any appropriate step length can be used for ease of implementation. Let us present the unknown coefficients of Padé approximation functions for each variable $v \in \{S, I, R\}$ by a point $\boldsymbol{x}_v = (a_{v0},\ a_{v1}, \ldots, a_{vM_v},\ b_{v0},\ b_{v1},\ b_{v2}, \ldots, b_{vM_v}) \in \mathbb{R}^{M_v+N_v+2}$, then there is a total number of $n = M_S + N_S + M_I + N_I + M_R + N_R + 6$ of unknown coefficients. Representing the corresponding approximate solutions and their derivatives by p_{vr}, p'_{vr} at $t_r \in \{t_0,\ t_1,\ t_2,\ t_3, \ldots,\ t_K\}$ and then substituting in Eqs. (1–3) we get a system of $3 \times (K+1)$ nonlinear algebraic equations. Let us define real-valued residual functions $\varepsilon_S(\boldsymbol{x}, t),\ \varepsilon_I(\boldsymbol{x}, t)$ and $\varepsilon_R(\boldsymbol{x}, t)$ of vector $\boldsymbol{x} = (\boldsymbol{x}_S,\ \boldsymbol{x}_I,\ \boldsymbol{x}_R) \in \mathbb{R}^n$ of unknown Padé approximation coefficients at any time $t \in [0, \infty)$. From (1–3), at each $t_r \in \{t_0,\ t_1,\ t_2,\ t_3, \ldots,\ t_K\}$ we get the following residuals from:

$$\varepsilon_S(\boldsymbol{x}, t_r) = \frac{A'_{Sr} - p_{Sr}B'_{Sr}}{B_{Sr}} - \mu N + \frac{\beta A_{Sr}A_{Ir}}{B_{Sr}(B_{Ir} + \alpha A_{Ir})} + \mu\frac{A_{Sr}}{B_{Sr}} \tag{4}$$

$$\varepsilon_I(\boldsymbol{x}, t_r) = \frac{A'_{Ir} - p_{Ir}B'_{Ir}}{B_{Ir}} - \frac{\beta A_{Sr}A_{Ir}}{B_{Sr}(B_{Ir} + \alpha A_{Ir})} + (\gamma + \mu)\frac{A_{Ir}}{B_{Ir}} \tag{5}$$

$$\varepsilon_R(\boldsymbol{x}, t_r) = \frac{A'_{Rr} - p_{Rr}B'_{Rr}}{B_{Rr}} - \gamma\frac{A_{Ir}}{B_{Ir}} + \mu\frac{A_{Sr}}{B_{Sr}} \tag{6}$$

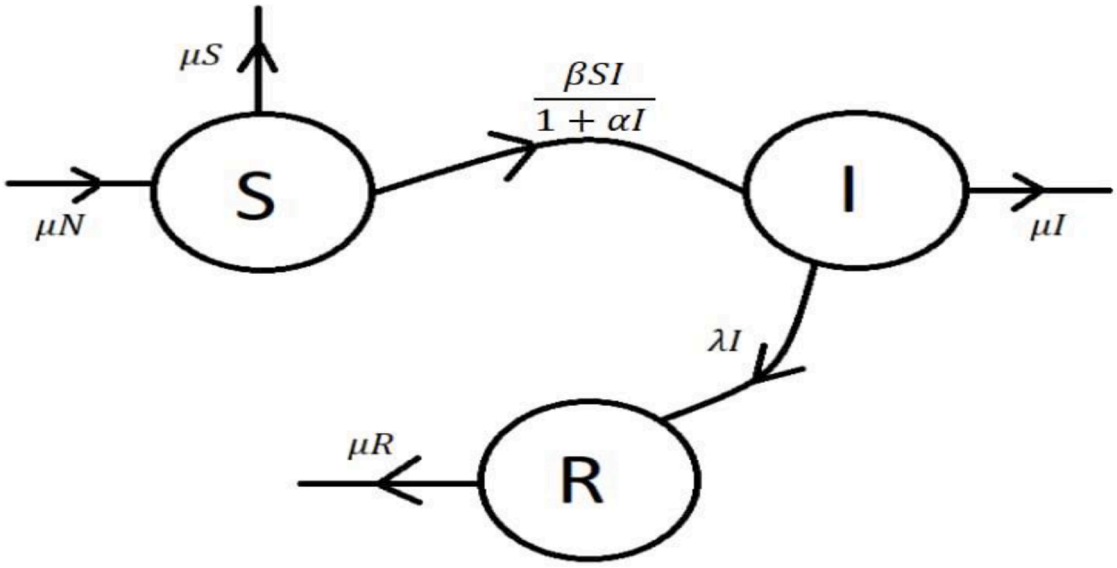

Fig. 1. Flow diagram of Covid-19 model with crowding effect [29].

(I) *Handling initial conditions as problem constraints*

The initial conditions and the physical restrictions give rise to the following equality and non-negativity constraints functions.

$$H_S(\boldsymbol{x}) = p_S(t_0) - S_0 = 0 \tag{7}$$

$$H_I(\boldsymbol{x}) = p_I(t_0) - I_0 = 0 \tag{8}$$

$$H_R(\boldsymbol{x}) = p_R(t_0) - R_0 = 0 \tag{9}$$

$$g_{vr}(\boldsymbol{x}) = p_v(t_r) \geq 0, \forall\ v \in \{S, I, R\} \ \text{ and } t_r \in \{t_0,\ t_1,\ t_2,\ t_3, \ldots,\ t_K\}. \tag{10}$$

(I) *Formulation of unconstrained global optimization problem*

The Padé approximation-based mathematical modeling of the underlying problem aims to find optimized decision vector $\boldsymbol{x} = (\boldsymbol{x}_S,\ \boldsymbol{x}_I,\ \boldsymbol{x}_R) \in \mathbb{R}^n$ of unknown coefficients so that the residuals at each discrete time step are minimized by meeting all the problem constraints. It can be observed from Eqs. (7–10) that the residual functions are highly nonlinear and hence lead to a highly nonlinear optimization problem. Due to the high complexity of the resulting optimization problem, an efficient optimizer is needed to be used. Evolutionary algorithms are modern methods that are believed to be less sensitive to the nature of the underlying problem, but they require the problem to be unconstrained. For this purpose, we use the penalty function approach to embed problem constraints into the objective function. Let L be a large positive real number and $P(\boldsymbol{x})$ be the function of the following relation.

$$P(\boldsymbol{x}) = \max\{0, |H_S(\boldsymbol{x})|, |H_I(\boldsymbol{x})|, |H_R(\boldsymbol{x})|, -g_S(\boldsymbol{x}), -g_I(\boldsymbol{x}),\ -g_R(\boldsymbol{x})\}.$$

Then the following unconstrained minimization problem is obtained

$$\textit{Minimize}\ \psi(\boldsymbol{x}) = \frac{1}{3(K+1)} \sum_{r=0}^{K} \left(\sum_{v \in \{S,I,R\}} [\varepsilon_v(\boldsymbol{x}, t_r)]^2 \right) + L \times P(\boldsymbol{x}). \tag{11}$$

3.2. Differential evolution (DE) global search optimizer

DE algorithm [49] is a population-based random search algorithm that starts with a randomly generated set of several solutions known as population. DE algorithm tries to improve the current population by developing new solutions through mutation and crossover evolutionary operations. The individual of the population with the smallest objective function value is termed as the best solution. The iteration process of the DE algorithm continues until a preset criterion is satisfied. The standard DE algorithm uses only three parameters to work that are (i) the population size $\kappa \in \mathbb{N}$ (ii) crossover rate $c_r \in [0, 1]$ and (iii) differential weight $\zeta > 0$. Geometric view of DE operations is shown in Fig. 2(a). Several studies describe the classic DE algorithm, also referred to as DE/rand/1/bin, in precise and smarter forms. We have implemented the traditional DE algorithm as Price, Storn and Lampinen explained in a detailed study [59] of the DE algorithm. To minimize a function of the form $\psi : \mathbb{R}^n \rightarrow \mathbb{R}$, the sequence of operations of classic DE algorithm [59] is given below:

1. Initialization

- The parameters κ, c_r and ζ are set. A positive integer T_{max} as a maximum number of iterations is also fixed. The iteration counter τ is initiated as $\tau = 0$.
- A population of κ solutions $\{\boldsymbol{x}_j = (x_j^1, x_j^2, x_j^3, \ldots, x_j^n) \in \mathbb{R}^n; 1 \leq j \leq \kappa\}$ is generated randomly.
- The κ solutions are evaluated i. e. $\psi_j = \psi(\boldsymbol{x}_j)\ \forall j = 1, 2, 3, \ldots, \kappa$. The best solution $\boldsymbol{x}^{best} = arg(\min\{\psi_j : 1 \leq j \leq \kappa\})$ is preserved.

2. Iterative process

- Set $\tau = \tau + 1$.
- For each target solution $\boldsymbol{x}_j, j \in \{1,2,3,\ldots,\kappa\}$, choose mutually distinct indices $j_1, j_2, j_3 \in \{1,2,3,\ldots,\kappa\} \backslash \{j\}$.
- Construct mutant vector $\boldsymbol{u}$ using differential mutation according as $\boldsymbol{u} = \boldsymbol{x}_{j_1} + \zeta \times (\boldsymbol{x}_{j_2} - \boldsymbol{x}_{j_3})$.
- Apply uniform/discrete crossover as:

For each dimension $i = 1, 2, 3, \ldots, n$, choose a random integer $j_{rand} \in \{1, 2, 3, \ldots, n\}$ and generate a uniformly distributed random number $i_{rand} \in (0, 1)$ to find a trial solution $\boldsymbol{y} = (y^i, y^2, y^3, \ldots, y^n) \in \mathbb{R}^n$ with coordinates:

$$y^i = \begin{cases} u^i, & \text{if } i_{rand} \leq c_r \text{ or } i = j_{rand} \\ x_j^i, & \text{otherwise}. \end{cases}$$

If $\psi(\boldsymbol{y}) > \psi_j$ discard $\boldsymbol{y}$ otherwise $\boldsymbol{x}_j \leftarrow \boldsymbol{y}$ and $\psi_j \leftarrow \psi(\boldsymbol{y})$.

- Update the best solution as: If $\psi_j \leq \psi(\boldsymbol{x}^{best})$ then $\boldsymbol{x}^{best} \leftarrow \boldsymbol{x}_j$.

3. Termination criterion

If $\tau < T_{max}$, then repeat step 2; otherwise, display the best solution and stop.

4. Optimum results

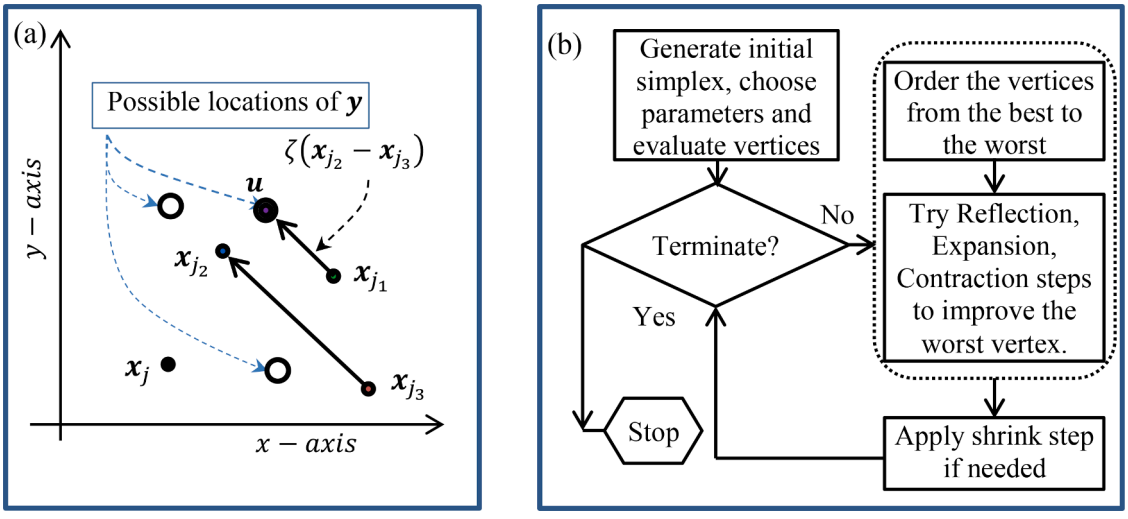

Fig. 2. (a) Geometry of DE algorithm in $\mathbb{R}^2$ (b) Schematic flowchart of NMS method.

Display x^{best} and $\psi(x^{best})$ as the optimum solution to the problem.

3.3. Nelder-Mead simplex (NMS) local optimizer

Nelder-Mead Simplex (NMS) algorithm [61] is a well-practiced gradient-free optimization method. For an n-dimensional problem, the NMS method starts with an initial n-simplex having non-zero volume. An n-simplex is a convex hull of points $x_1, x_2, \ldots, x_{n+1}$ in $\mathbb{R}^n$. The vertices are ordered from the best to the worst according to as $\psi(x_1) \leq \psi(x_2) \leq \psi(x_2) \leq \ldots \leq \psi(x_{n+1})$. At each iteration, the centroid $G = \frac{1}{n}\sum_{j=1}^{n} x_j$ of all the non-worst vertices is computed. Then the operations of reflection, expansion, and contractions about G are used to replace the worst vertex. In case of failure, the simplex is squeezed towards the best vertex using shrink operation. The equations of four NMS operations are given below.

(i) *Reflection*: $y = x_{n+1} + \alpha \times (G - x_{n+1})$.
(ii) *Expansion*: $y = x_{n+1} + \beta \times (G - x_{n+1})$.

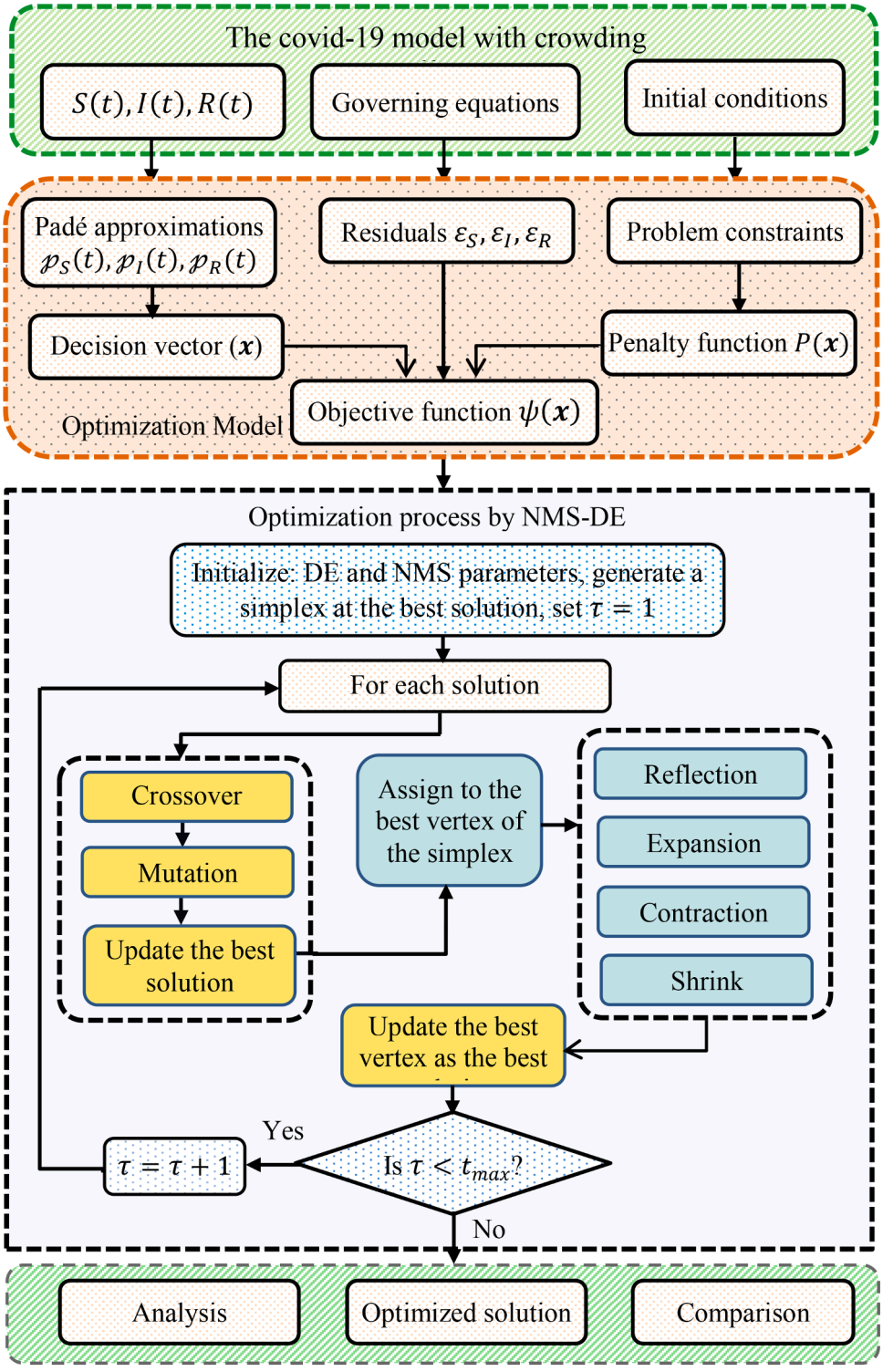

Fig. 3. Schematic flowchart of the proposed EPA scheme.

(iii) *Contraction outside*: $\boldsymbol{y} = \boldsymbol{x}_{n+1} + \gamma \times (\boldsymbol{G} - \boldsymbol{x}_{n+1})$.

Contraction inside: $\boldsymbol{y} = \boldsymbol{x}_{n+1} - \gamma \times (\boldsymbol{G} - \boldsymbol{x}_{n+1})$.

(i) *Shrink*: $\boldsymbol{x}_j = \boldsymbol{x}_j + \delta \times (\boldsymbol{x}_1 - \boldsymbol{x}_j)\ \forall\, j = 2, 3, \ldots, n+1$.

The typical values of these parameters in the original study [61] are $\alpha = 2,\ \beta = 3, \gamma = \delta = 0.5$. We use a non-stagnated convergent variant of the NMS method proposed by Ali et al. [60]. The order of operations of the NMS method is outlined as a flowchart presented in Fig. 2(b). The complete schematic framework of the proposed EPA scheme for the underlying model is presented in Fig. 3.

4. Results and discussion

This section consists of essential components of the current work. The principal objective of the present study is to obtain the semi-analytical solution of the considered model with high accuracy and preserve vital properties of the dynamics of the model. It is imperative to investigate the EPA scheme's accuracy, efficiency, and reliability when applied to the considered model. Therefore, in the following subsections, we conduct a twofold study of the solution obtained by the EPA scheme. Firstly, we analyze the optimization results of our proposed EPA scheme. Secondly, we compare the solutions obtained by the EPA scheme with a well-practiced nonstandard finite difference (NSFD) scheme to highlight the prominent aspects of the proposed method.

4.1. Analysis of optimization results

We observe that the global minimum value of the objective function $\psi(\boldsymbol{x})$ defined by Eq. (11) is zero, which corresponds to a global optimal point $\boldsymbol{x}^*$. Keeping in mind the positivity of residual functions $\varepsilon_S(\boldsymbol{x}, t)$, $\varepsilon_I(\boldsymbol{x}, t)$, $\varepsilon_R(\boldsymbol{x}, t)$ and the penalty function $P(\boldsymbol{x})$ for all t and $\boldsymbol{x}$, we have that:

$$\psi(\boldsymbol{x}^*) = 0 \Leftrightarrow \varepsilon_v(\boldsymbol{x}^*, t) = 0\ \forall\ v \in \{S, I, R\} \text{ and } P(\boldsymbol{x}^*) = 0.$$

The equation $\varepsilon_v(\boldsymbol{x}^*, t) = 0$ implies that $\boldsymbol{x}^*$ is the exact solution of the governing equation of $v \in \{S,I,R\}$, whereas $P(\boldsymbol{x}^*) = 0$ guarantees that all initial conditions and the mentioned structure-preserving properties of the model are accurately satisfied.

The proposed EPA scheme tries to find the approximate solution, say $\boldsymbol{x}^{**}$, of the model with acceptable accuracy. Hence the objective of the optimization process is to minimize $\psi(\boldsymbol{x})$ as much as possible by ensuring that all problems constraints are satisfied. To optimize the formulated problem by NMS-DE, the parameters used in the proposed EPA scheme have been presented in Table 1.

The optimal values of the Padé approximation coefficients have been found under various options of orders Padé approximations at endemic and disease-free equilibrium states. To validate the performance of the proposed hybrid optimizer reasonably and explore the interpolating strength of Padé approximants, we have considered Padé rational functions of orders (4, 4), (5, 5) and (6, 6) to approximate each state variable for endemic as well as disease-free equilibrium. Table 2 presents the statistical measures (best, mean, and standard deviation (SD)) of optimization results of $\psi(\boldsymbol{x})$ produced by the proposed hybrid optimizer in 20 independent runs. Mean convergence curves of 2000 iterations of optimization progress using (4, 4), (5, 5), and (6, 6) order approximants have been exhibited in Fig. 4.

Tables 3 and 4 represent the optimum values of unknown coefficients, which belong to the smallest optimal values of the objective function over 20 runs.

In the following subsections, the optimization results are presented and analyzed as:

Table 1
EPA parameters.

Parameter	Description	Value	Reference
κ	Population size for DE algorithm	50	[49, 59]
c_r	The crossover acceptance rate of DE algorithm	0.9	[49, 59]
ζ	Differential weight of DE algorithm	0.5	[49, 59]
T_{max}	Maximum number of iterations for DE algorithm to produce the optimum solution	2000	Assumed
(M_v, N_v)	Order of Padé approximation for state variable v	(4,4), (5,5), (6,6)	
n	Problem dimension denoting the number of unknown Padé approximation coefficients	$\sum_{v\in\{S,I,R\}} (M_v + N_v)$	
L	The penalty factor of penalty function	10^6	
μ	Death rate	0.1	[29]
β	Bilinear incidence rate	0.2464 (EE) 0.1464 (DFE)	[29]
γ	Recovered rate	0.07	[29]
α	Infection rate	0.01	[29]
$V_{threshold}$	The threshold value for convergence speed	10^{-04}	Assumed

Table 2
Optimization results for two equilibrium states.

Order	DFE			EE		
	Best	Mean	SD	Best	Mean	SD
(4,4)	2.5e-07	**8.1e-06**	4.9e-04	8.9e-08	8.9e-06	3.1e-05
(5,5)	**1.7e-11**	3.6e-05	1.1e-05	4.2e-09	**1.2e-05**	1.6e-05
(6,6)	8.4e-07	9.4e-06	**5.3e-06**	**3.7e-08**	5.7e-05	**7.1e-06**

(i) The accuracy of the solution is assessed by the fact that how small $\psi(\boldsymbol{x}^{**})$ is found.
(ii) Consistency of NMS-DE algorithm demonstrated by computing best, mean and standard deviations of final optimal values over several optimizer attempts.
(iii) The convergence speed of NMS-DE is assessed by many iterations used to achieve a threshold value denoted by $_{the\ V\ threshold}$.
(iv) The effectiveness of the proposed method is justified by comparing the obtained solutions with multiple modern metaheuristics.

4.1.1. Accuracy

From Table 2, we observe that the best minimum values of $\psi(\boldsymbol{x}^{**})$ ranges from 2.5e-07 to 1.7e-11 at DFE point and lie in the range [3.7e-08, 4.2e-09] at EE point for various orders of Padé approximants. Figs. 5–7 present the squared residuals of governing equations of state variables over a time of up to 150 days. One can observe from figures that the squared residuals can be minimized up to sufficiently small values 10e-15. Moreover, Fig. 5 shows that the solutions of governing equation of susceptible population achieve accuracies below 10e-6. In contrast, Fig. 6 shows that the accuracy of an infected population is below 10e-10 at both the equilibrium points and for all orders of the Padé approximants. Similarly, the accuracy of solutions of governing equation of susceptible population falls around 10e-10 and 10e-06 at DFE and EE points, respectively. These results ensure that the solutions found by the EPA scheme can achieve approximate solutions of the model with good accuracies.

4.1.2. Consistency and reliability

To assess the consistency of NMS-DE, we do not rely on the solution achieved by a single run of the optimizer. To investigate the reliability of the results, we perform a statistical analysis of marks obtained in multiple runs of the NMSE-DE algorithm. The results presented in Table 2

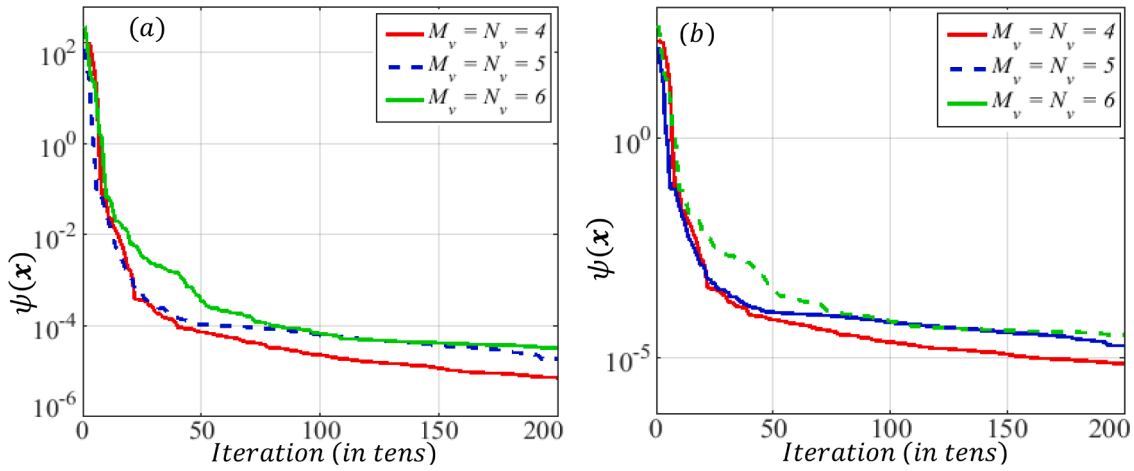

Fig. 4. Mean convergence curves of DE-NMS at (a) DFE (b) EE state.

Table 3
Optimal values of coefficients at DFE state.

Order	i	a_{Si}	b_{Si}	a_{Ii}	b_{Ii}	a_{Ri}	b_{Ri}
(4,4)	0	0.5	1	0.2	1	0.3	1
	1	11.62412	23.19136	−0.4410504	−1.99006	4.518759	15.1704
	2	17.96686	27.99012	21.62841	129.7301	41.81043	151.2964
	3	−4.589881	−4.792515	−0.5847947	−40.31095	−0.7980348	−13.7038
	4	3.214352	3.215415	0.0045273	71.09928	0.0038315	14.43962
(5,5)	0	0.5	1	0.2	1	0.3	1
	1	1.3390699	2.6037853	0.7072810	3.7697691	2.1501625	7.2888593
	2	788.49054	1570.245	−0.8496248	−5.7637786	1.4227432	4.0616136
	3	10.919599	36.620152	9.3823315	56.037332	7.9462428	30.799049
	4	4.7504681	3.9790506	−0.1915813	−7.5008662	−0.152888	−2.5337034
	5	4.7330172	4.7324437	0.0001154	5.4266051	−0.0001095	0.7767076
(6,6)	0	0.5	1	0.2	1	0.3	1
	1	1.08109	2.0329	1.2794	6.50122	0.452094	1.55232
	2	3.2641	8.91808	8.57519	47.9268	1.48791	5.34671
	3	10.8111	10.5012	6.6515	31.3825	6.66342	21.5409
	4	8.40516	26.7405	0.304318	20.9876	5.69837	24.053
	5	2.10008	1.75478	−0.0081925	−1.98912	−0.119462	−1.33771
	6	1.41142	1.41119	9.945e-05	1.2269	6.887e-05	0.603988

Table 4
Optimal values of coefficients at EE state.

Order	i	a_{Si}	b_{Si}	a_{Ii}	b_{Ii}	a_{Ri}	b_{Ri}
(4,4)	0	0.5	1	0.2	1	0.3	1
	1	1.962976	3.873777	10.50587	52.57363	4.722648	115.74965
	2	5.110822	9.836035	16.82871	96.37293	32.34391	111.6259
	3	−0.2354903	−0.3935344	−14.07242	−77.26163	−0.5267137	−1.305307
	4	0.561096	0.8118427	3.553253	19.55911	.082824	8.514212
(5,5)	0	0.5	1	0.2	1	0.3	1
	1	−0.2527975	−0.5398225	4.208253	21.04604	2.752185	9.216065
	2	21.55926	43.33501	1.465227	11.21728	17.88936	64.84665
	3	71.79745	139.7148	−7.792861	−44.28272	16.88882	54.20429
	4	3.595083	4.53876	2.867689	15.78287	1.212053	11.0835
	5	8.729702	12.6298	1.85344	10.20357	0.6390833	5.025223
(6,6)	0	0.5	1	0.2	1	0.3	1
	1	−2.70156	−5.4178	4.88544	24.4964	7.69363	25.8147
	2	−6.08778	−12.5332	0.197156	8.6703	11.8406	39.6912
	3	−4.29643	−4.72722	9.74047	28.7846	9.08754	50.9515
	4	−8.35969	−17.1982	8.09084	66.408	7.75748	15.1099
	5	3.24166	4.79335	−0.899575	−5.46805	−0.0815287	0.269303
	6	−2.99372	−4.33166	1.66903	9.18781	1.07708	8.47145

describe that the mean of the optimal value of $\psi(x^{**})$ remains within the range [8.1e-06, 5.7e-05] for all considered orders and at both equilibrium points with corresponding range [5.3e-06, 4.9e-04] for standard deviations. These facts and figures demonstrate that the performance of NMS-DE in optimization tasks is consistent, and results are reliable with good accuracy.

4.1.3. Convergence speed

Fig. 4 presents the mean convergence curves of the optimization process at two equilibrium points for all orders of Padé approximants.

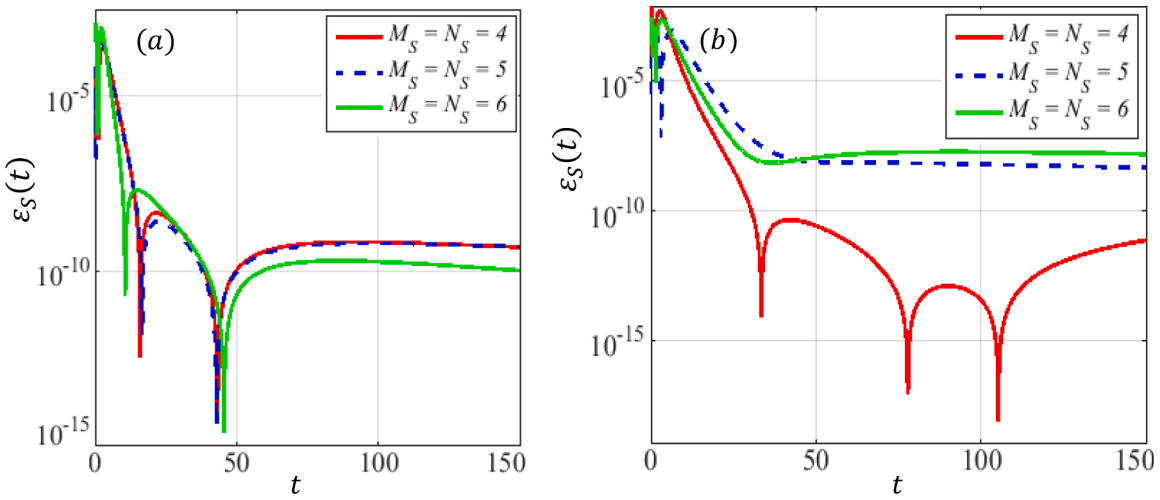

Fig. 5. Squared residuals of governing equation of class S at (a) EE (b) DFE state.

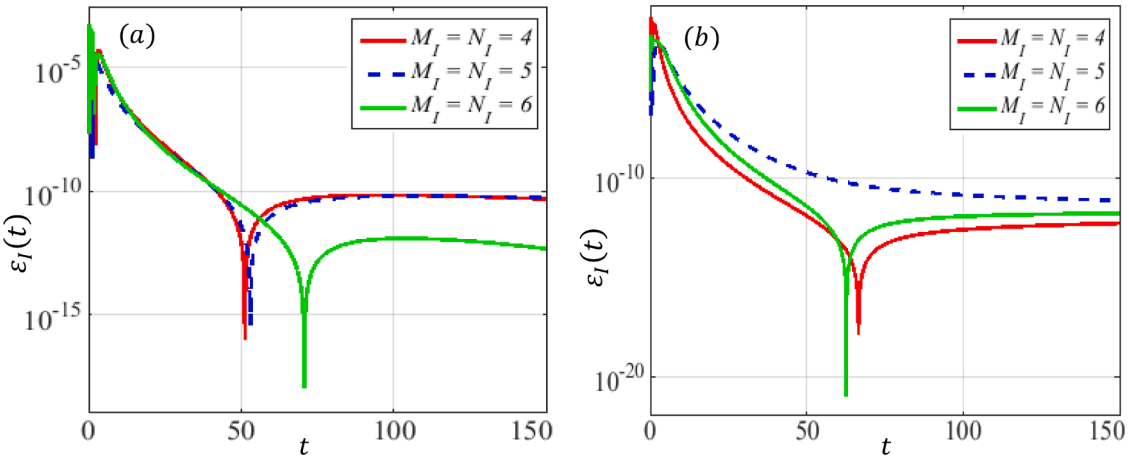

Fig. 6. Squared residuals of governing equation of class I at (a) EE (b) DFE state.

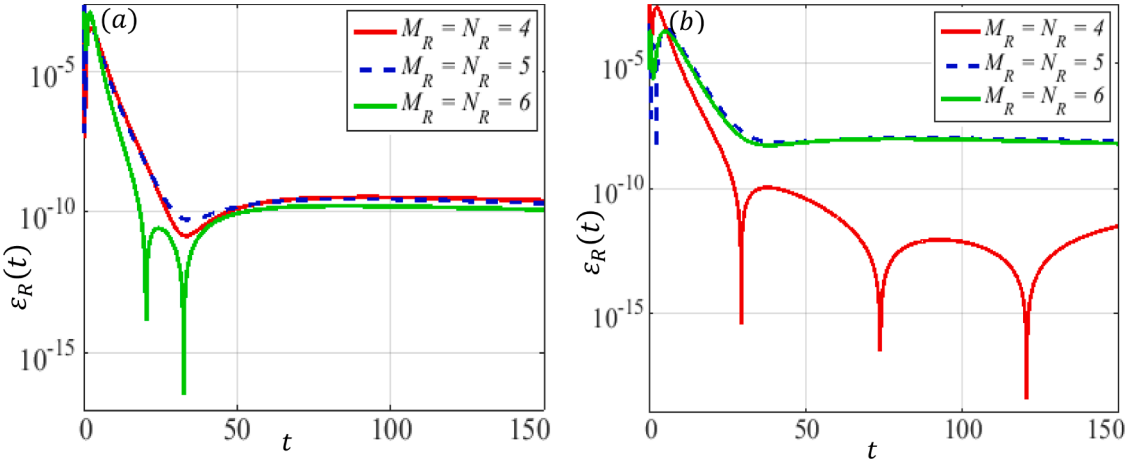

Fig. 7. Squared residuals of governing equation of class R at (a) EE (b) DFE state.

We can observe from Fig. 4(a) that, at DFE point, the threshold value $V_{threshold}$ is achieved in less than 500, 600, and 900 iterations on average for (4, 4), (5, 5), and (6,6) order solutions respectively. Similarly, $V_{threshold}$ is achieved in around 400, 500, and 750 iterations (please see Fig. 4(b)) for (4, 4) in corresponding solutions at EE point. These observations highlight that the order of Padé approximants is directly proportional to computational cost and speed of convergence.

4.1.4. *Performance comparison with other metaheuristics*

In this subsection, we present a comparison of the optimization re-

sults of our proposed method with original DE and NMS algorithms and with a few modern metaheuristics under the same settings of population size, the maximum number of iterations, and the threshold value. The other built-in parameters of all competing algorithms are kept the same as recommended in their original propositions. The metaheuristics used for comparison are Teaching-Learning Based Optimization (TLBO) [47], Particle Swarm Optimization (PSO) [48], DE [49], Controlled Showering Optimization (CSO) [52], Water Cycle Algorithm (WCA) [53], Artificial Bee Colony (ABC) [55] and grey Wolf Optimizer (GWO) [56]. Tables 5 and 6 exhibit the best minimum value, percentage (P%) of successful runs to achieve $V_{threshold}$, and an average number of iterations (T_a) in successful runs to achieve $V_{threshold}$ over 20 independent runs of each algorithm that are used as performance measures to compare the results of all competing metaheuristics.

The features of results presented in Tables 5 and 6 are comprised of six test instances of solutions of various Padé approximants' orders at two equilibrium points. We observe that due to significant dependency on provided initial guesses and the complexity of the underlying problem, the performance of the NMS algorithm is nowhere comparable to all other global search algorithms. Hence we exclude NMS results from further comparative analysis. One can observe from these results that the metaheuristics WCA, ABC, and GWO were unsuccessful in achieving the threshold value $V_{threshold}$ in all attempts and returned poor approximations of optimum values. Their mutual comparison is based on the best objective function values only. WCA was able to minimize the objective function better than ABC and GWO. Therefore, further competition occurs between TLBO, PSO, DE, and CSO, and NMS-DE algorithms.

Comparing the results of TLBO, PSO, DE, CSO, and NMS-DE, the following vital facts can be observed:

1 The DE algorithm computed the best minimum objective function values are better than TLBO, PSO, and CSO for all test instances. The best minimum values found by NMS-DE are far better than those of all of its competitors. The optimal values found by NMS-DE are 92.42%, 99.998%, and 90.34% better than those of the DE algorithm for respective cases of DFE point. At EE point, NMSE found 85.41%, 99.65%, and 99.36% better values than the DE algorithm for three respective cases of endemic equilibrium.
2 NMS-DE algorithm outperformed other metaheuristics in the sense of success rates (100%) of achieving pre-set accuracy $V_{threshold}$ in all scenarios. On the other hand, none of the competing metaheuristics achieved such a consistent performance while solving the formulated optimization problem of the CovidCE model. For the 5th order solution at DFE point and 6th order solution at EE point, only TLBO showed success rates of 74% and 71%, respectively, better than those of DE, but DE outperformed TLBO, PSO, and CSO on the rest of the cases. This observation justifies the selection of DE as a global solver and the need for further hybridization to achieve a more efficient hybrid solver (NMS-DE).
3 The final notable point is the speed of convergence of the proposed NMS-DE is faster than those of TLBO, PSO, DE, and CSO. The computational cost is measured by the number of iterations required to achieve the threshold value $V_{threshold}$. At DFE point, NMS-DE consumed around 413 (20.65%), 668 (33.4%), and 891 (44.55%) iterations for 4th, 5th, and 6th order solution, respectively. At EE point these amounts are 973 (48.65%), 1023 (51.15%) and 1274 (63.2%) respectively. Fig. 8 presents the competitive percentage measure of the faster or slower convergence speed of NMS-DE over each successful metaheuristic. The positive and negative percentages reflect that the convergence speed of NMS-DE is faster or slower than a competing algorithm. The convergence speed of NMS-DE is better than all of the competitors except for the 6th order solution at EE point, where TLBO was better than NMS-DE.

4.2. Model simulations

The graphical views of evolutions of subpopulations of the underlying model are presented in Fig. 9–11. One can observe that the optimized solutions found in be EPA scheme for all considered orders of Padé approximants at both equilibrium points converge exactly to steady-state points. This fact reflects that solution by EPA scheme is in good agreement with that of the NSFD method in the vicinity of equilibrium points [62]. It is worth mentioning that the convergence speed of EPA-based solutions is significantly faster than those of NSFD; we may also observe that the model's physically vital properties like positivity, boundedness, dynamical consistency, and converges to actual steady states (disease-free and endemic equilibria) are also preserved by EPA scheme. Furthermore, the proposed scheme is also independent of the choice of step lengths and unconditionally converges to both states of the model.

5. Conclusions

The context of the current study is the evolvement of an evolutionary solver for a complex Covid-19 with a crowding effect (CovidCE) model. The main focus of this research was the formulation and solution of the underlying CovidCE model as an equivalent global optimization problem. This work is a blend of mathematical programming, epidemiology, and metaheuristics. The first contribution relates to the theory of optimization that includes two prominent innovations (i) formulation of a new general order Padé approximation based equivalent global optimization problem preserving vital properties (positivity, boundedness, and stability) of the CovidCE model. This generalization allows varying or adjusting the orders of Padé approximants for approximating the solution more accurately (ii) The formulated optimization problem's complexity barred not only the use of deterministic optimizers but also modern metaheuristics. Therefore, the second contribution of this work was to tune a new hybrid method, named NMS-DE, to solve the formulated problem. This step was accompanied by a statistical analysis of the results of various orders of solutions. The comparative analysis witnessed that the proposed hybrid method handled the optimization phase of the EPA scheme efficiently and outperformed other metaheuristics in terms of accuracy, consistency, and speed of convergence.

Table 5
Optimization results of competing metaheuristics at DFE point.

Algorithm	(4, 4) order solution			(5, 5) order solution			(6, 6) order solution		
	Best	P%	T_a	Best	P%	T_a	Best	P%	T_a
TLBO	1.4e-04	58	1078	5.3e-05	74	1142	1.5e-06	68	1212
PSO	3.8e-06	64	1685	1.0e-06	31	1715	7.1e-05	48	1729
DE	3.3e-06	71	1011	9.2e-07	70	1501	8.7e-06	81	1811
NMS	7.0e+06	0	–	3.5e+06	0	–	8.1e+06	0	–
CSO	7.1e-03	53	1623	4.6e-06	63	1495	5.6e-05	57	1677
WCA	5.1e-04	0	–	8.0e-04	0	–	1.4e-04	0	–
ABC	3.3e-01	0	–	2.2e00	0	–	9.1e-01	0	–
GWO	6.2e-02	0	–	2.8e-04	0	–	7.9e-03	0	–
NMS-DE	**2.5e-07**	**100**	**413**	**1.7e-11**	**100**	**668**	**8.4e-07**	**100**	**891**

Table 6
Optimization results of competing metaheuristics at EE point.

Algorithm	(4, 4) order solution			(5, 5) order solution			(6, 6) order solution		
	Best	*P*%	T_a	Best	*P*%	T_a	Best	*P*%	T_a
TLBO	2.3e-05	60	1053	1.7e-05	70	1083	1.5e-05	71	**976**
PSO	4.6e-06	60	1723	2.1e-05	20	1690	1.5e-05	70	1729
DE	6.1e-07	64	1303	1.2e-06	73	1429	5.8e-06	68	1691
NMS	3.4e+08	0	–	5.9e+06	0	–	7.7e+06	0	–
CSO	5.1e-05	50	1225	3.7e-05	60	1551	5.6e-05	60	1677
WCA	2.9e-04	0	–	4.0e-04	0	–	9.1e-04	0	–
ABC	4.0e00	0	–	1.8e00	0	–	2.4e01	0	–
GWO	3.7e-02	0	–	9.1e-03	0	–	1.5e-02	0	–
NMS-DE	**8.9e-08**	**100**	**973**	**4.2e-09**	**100**	**1023**	**3.7e-08**	**100**	1264

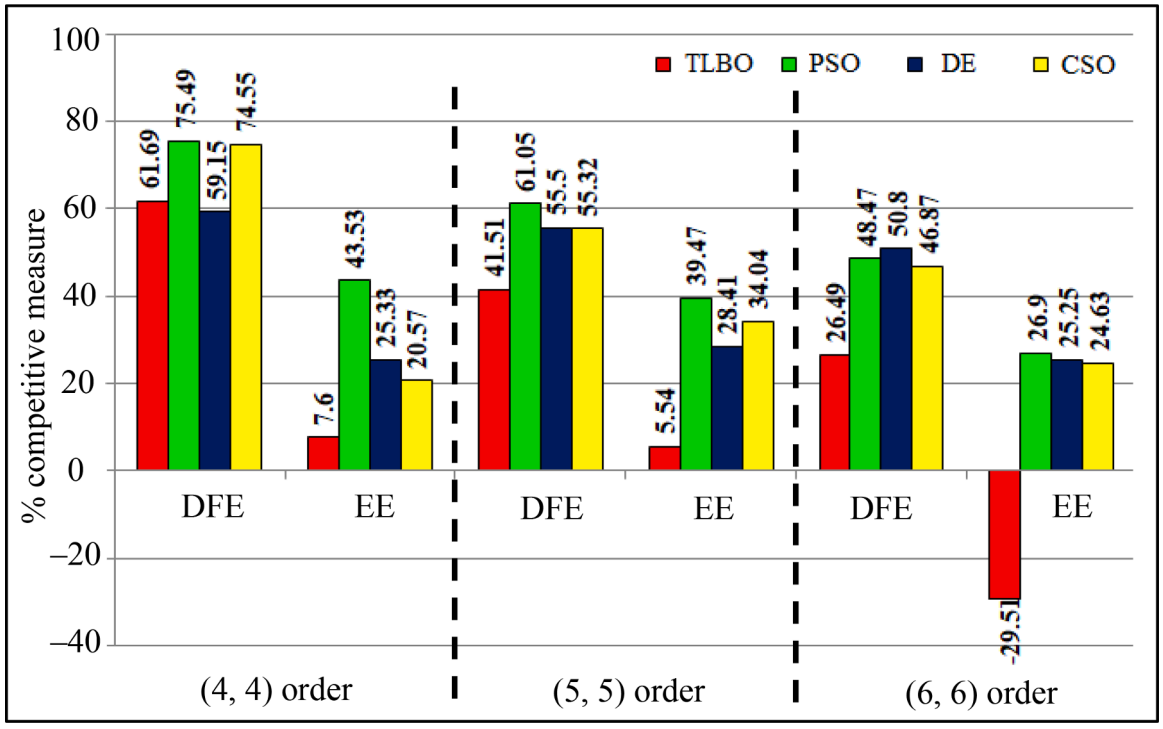

Fig. 8. Percentage competitive measures of convergence speed of NMS-DE.

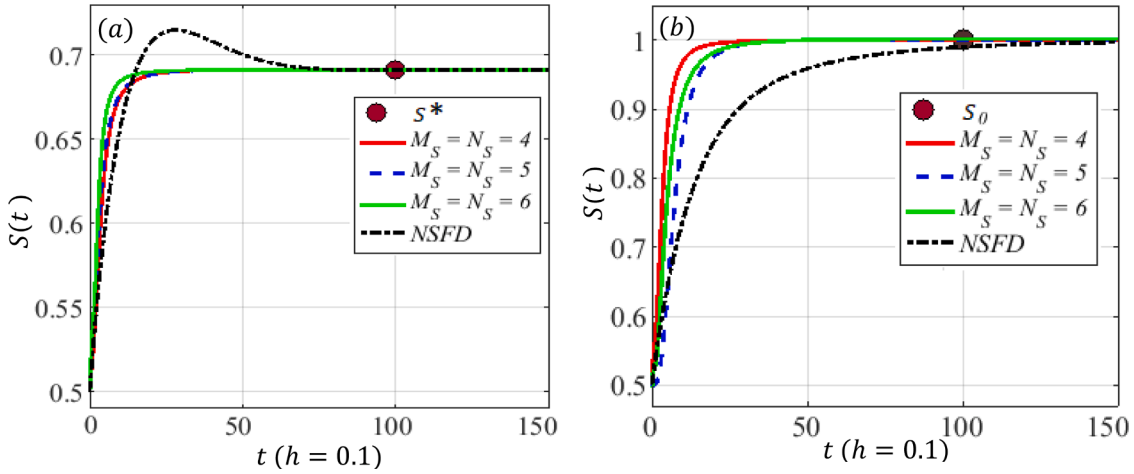

Fig. 9. Dynamics of susceptible population at (a) EE (b) DFE states.

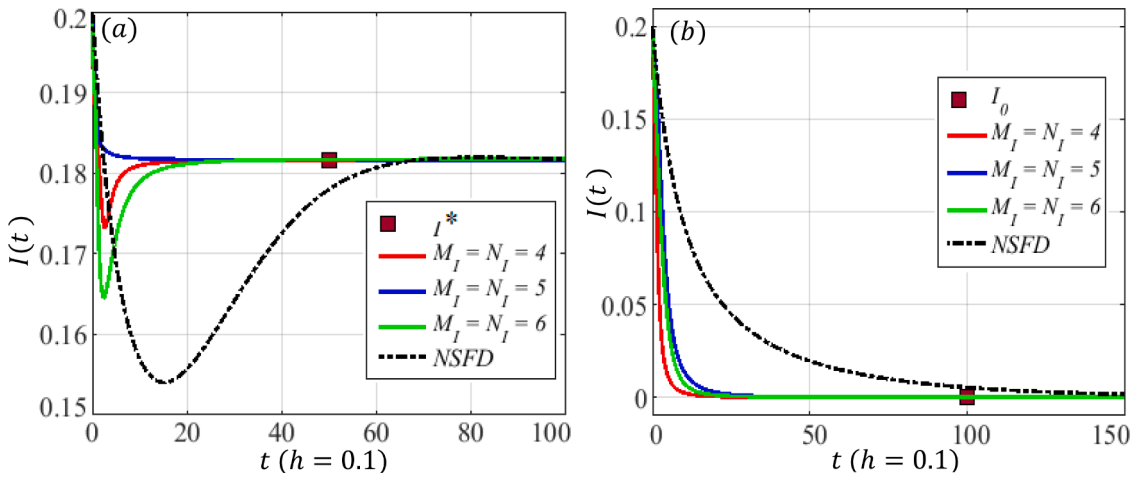

Fig. 10. Dynamics of Infected population at (a) EE (b) DFE states.

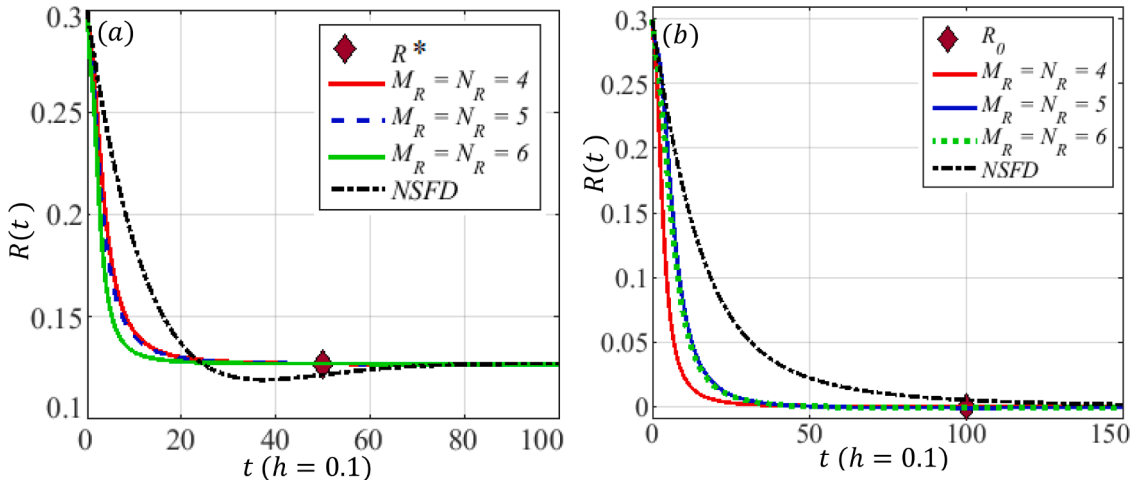

Fig. 11. Dynamics of the recovered population at (a) EE (b) DFE states.

The Final contribution relates to the characteristics of the obtained solution of the CovidCE model. To the best of our knowledge, the exact analytical solution of such epidemiological models with all physical properties has not been reported so far. The current work enables us to observe an approximate closed-form solution of the CovidCE type model. The graphics of model simulations also reveal that the solution found by the EPA scheme is in good agreement with NSFD in convergence to equilibrium points and possesses a notably faster convergence speed.

Conflict of interest and authorship conformation form

Please check the following as appropriate:

- All authors have participated in (a) conception and design, or analysis and interpretation of the data; (b) drafting the article or revising it critically for important intellectual content; and (c) approval of the final version.
- This manuscript has not been submitted to, nor is under review at, another journal or other publishing venue.
- The authors have no affiliation with any organization with a direct or indirect financial interest in the subject matter discussed in the manuscript

CRediT authorship contribution statement

Javaid Ali: Conceptualization, Methodology. **Ali Raza:** Data curation, Writing – original draft. **Nauman Ahmed:** Data curation, Writing – original draft. **Ali Ahmadian:** Supervision, Validation, Writing – review & editing, Writing – original draft. **Muhammad Rafiq:** Writing – review & editing, Validation. **Massimiliano Ferrara:** Writing – review & editing, Validation.

References

[1] Zeb A, Alzahrani E, Erturk VS, Zaman G. Mathematical model for coronavirus disease 2019 (Covid-19) containing isolation class. Biomed Res Int 2020;10:1–7.
[2] Riyapan P, Shuaib SE, Intarasit A. A mathematical model of covid-19 pandemic: a case study of bangkok, thailand. Comput Math Methods Med 2021;2021:1–11.
[3] Oud MAA, Ali A, Alrabaiah H, Ullah S, Khan MA, Islam S. A fractional-order mathematical model for covid-19 dynamics with quarantine, isolation, and environmental viral load. Advan Difference Equations 2021;2021:1–19.
[4] Shaikh AS, Shaikh IN, Nisar KS. A mathematical model of covid-19 using fractional derivative: outbreak in india with dynamics of transmission and control. Advan Difference Equations 2021;2020:1–19.
[5] Ahmed I, Modu GU, Yusuf A, Kumam P, Yusuf I. A mathematical model of coronavirus disease (Covid-19) containing asymptomatic and symptomatic classes. Results in Physics 2021;2021:1–15.
[6] Ullah S, Khan MA. Modelling the impact of non-pharmaceutical interventions on the dynamics of novel coronavirus with optimal control analysis with a case study. Chaos, Solitons Fractals 2020;2020:1–32.
[7] Peter OJ, Qureshi S, Yusuf A, Al-Shomrani M, Idowu AA. A new mathematical model of covid-19 using real data from pakistan. Results in Phy 2021;2021:1–10.

[8] Nazir G, Zeb A, Shah K, Saeed T, Khan RA, Khan SIU. Study of covid-19 mathematical model of fractional order via modified euler method. Alexandria Engineering Journal 2021;60:5287–96.
[9] Kyrychko YN, Blyuss KB, Brovchenko I. Mathematical modelling of the dynamics and containment of covid-19 in ukraine. Sci Rep 2020;10:1–17.
[10] Khoshnaw SH, Salih RH, Sulaimany S. Mathematical modelling for coronavirus disease (Covid-19) in predicting future behaviours and sensitivity analysis. Math Model Nat Phenom 2020;10:1–13.
[11] Sasmita NR, Ikhwan M, Suyanto S, Chongsuvivatwong V. Optimal control on a mathematical model to pattern the progression of coronavirus disease 2019 (Covid-19) in indonesia. Global Health Research and Policy 2020;5:1–12.
[12] Tiwari V, Bisht N, Deyal N. Mathematical modelling based study and prediction of covid-19 epidemic dissemination under the impact of lockdown in india. medRxiv 2020;6:1–16.
[13] Wang S, Tang W, Xiong L, Fang M, Zhang B, Chiu CY, Fan R. Mathematical modelling of transmission dynamics of covid-19. Big Data and Information Analytics 2021;6:12–25.
[14] Baek YJ, Lee T, Cho Y, Hyun JH, Kim MH, Sohn Y, Choi JY. A mathematical model of covid-19 transmission in a tertiary hospital and assessment of the effects of different intervention strategies. PLoS One 2020;15:1–10.
[15] Santaella-Tenorio J, Guerrero R, Bravo L. Mathematical model and covid-19 modelos matemáticos y el covid-19. Colomb. Med. 2020;51:1–12.
[16] Peter OJ, Shaikh AS, Ibrahim MO, Nisar KS, Baleanu D, Khan I, Abioye AI. Analysis and dynamics of fractional-order mathematical model of covid-19 in nigeria using atangana-baleanu operator. Computers, Materials and Continua 2020;66:1–20.
[17] Moyles IR, Heffernan JM, Kong JD. Cost and social distancing dynamics in a mathematical model of covid-19 with application to ontario, canada. medRxiv 2020;15:1–10.
[18] Krivorot'ko OI, Kabanikhin SI, Zyat'kov NY, Prikhod'ko AY, Prokhoshin NM, Shishlenin MA. Mathematical modelling and forecasting of covid-19 in moscow and novosibirsk region. Numer Anal Appl 2020;13:332–48.
[19] Harjule P, Tiwari V, Kumar A. Mathematical models to predict covid-19 outbreak: an interim review. J Interdiscip Math 2021;15:1–26.
[20] Kim BN, Kim E, Lee S, Oh C. Mathematical model of covid-19 transmission dynamics in south korea: the impacts of travel restrictions, social distancing, and early detection. Processes 2020;8:1–10.
[21] Diaz JEM, Raza A, Ahmed N, Rafiq M. Analysis of a nonstandardnonstandard computer method to simulate a nonlinear stochastic epidemiological model of coronavirus-like diseases. Comput Methods Programs Biomed 2021;204:1–10.
[22] Raza A, Ahmadian A, Rafiq M, Salahshour S, Laganà IR. An analysis of a nonlinear susceptible-exposed-infected-quarantine-recovered pandemic model of a novel coronavirus with delay effect. Results in Physics 2021;21:01–7.
[23] Zamir Muhammad, Shah Kamal, Nadeem Fawad, Bajuri Mohd Yazid, Ahmadian Ali, Salahshour Soheil, Ferrara Massimiliano, COVID-19 state of. Threshold conditions for global stability of disease free. Results in Physics 2021;21:103784.
[24] Gupta Vedika, Jain Nikita, Katariya Piyush, Adarsh Kumar, Mohan Senthilkumar, Ahmadian Ali, Ferrara Massimiliano. An emotion care model using multimodal textual analysis on COVID-19. Chaos, Solitons Fractals 2021;144:110708.
[25] Saha Pritam, Mukherjee Debadyuti, Singh Pawan Kumar, Ahmadian Ali, Ferrara Ram Sarkar. GraphCovidNet: a graph neural network based model for detecting COVID-19 from CT scans and X-rays of chest. Sci Rep 2021;11(1):1–16.
[26] Ahmad S, Ullah A, Shah K, Salahshour S, Ahmadian A, Ciano T. Fuzzy fractional-order model of the novel coronavirus. Adv Difference Equat 2020;2020:1–17.
[27] Ahmad N, Elsonbaty A, Raza A, Rafiq M, Adel W. Numerical simulation and stability analysis of a novel reaction-diffusion covid-19 model. Nonlinear Dyn 2021;23:01–18.
[28] Ghorui Neha, Ghosh Arijit, Mondal Sankar Prasad, Bajuri Mohd Yazid, Ahmadian Ali, Salahshour Soheil, Ferrara Massimiliano. Identification of dominant risk factor involved in spread of COVID-19 using hesitant fuzzy mcdm methodology. Results in physics 2021;21:103811.
[29] Shariq Mohd, Singh Karan, Bajuri Mohd Yazid, Pantelous Athanasios A, Ahmadian Ali, Salimi Mehdi. A secure and reliable rfid authentication protocol using digital schnorr cryptosystem for iot-enabled healthcare in COVID-19 scenario. Sustainable Cities and Society 2021;75:103354.
[30] Mateescu GD. On the application of genetic algorithms to differential equations. Romanian J Economic Forecasting 2006;2:5–9.
[31] Lee ZY. Method of bilaterally bounded to solution blasius equation using particle swarm optimization. Appl Math Comput 2006;179:779–86.
[32] Babaei M. A general approach to approximate solutions of nonlinear differential equations using particle swarm optimization. Appl Soft Comput 2013;13(7):3354–65.
[33] Karr CL, Wilson E. A self-tuning evolutionary algorithm applied to an inverse partial differential equation. Appl Intelligence 2003;19:147–55.
[34] Cao H, Kang L, Chen Y. Evolutionary modelling of systems of ordinary differential equations with genetic programming. Genetic Programming and Evolvable Machines 2000;1(4):309–37.
[35] Mastorakis Nikos E. Unstable ordinary differential equations: solution via genetic algorithms and the method of nelder-mead. WSEAS Trans Math 2006;5(12):1276–81.
[36] Pageant N, Bureerat S. Solving partial differential equations using a new differential evolution algorithm. Math Probl Eng 2014;2014(747490):10.
[37] Ali J, et al. Numerical treatment of nonlinear model of virus propagation in computer networks: an innovative evolutionary padé approximation scheme. Adv Difference Equations 2018;2018(1). 214.
[38] Nisar KS, Ali J, Mahmood MK, Ahmed D, Ali S. Hybrid evolutionary padé approximation approach for numerical treatment of nonlinear partial differential equations. Alexandria Engineering J 2021;60(5):4411–21.
[39] Baker GA. Essentials of padé approximants. New York, NY, USA: Academic Press; 1975.
[40] Baker G.A., Morris P.G., Padé approximants, Addison-Wesley, 1981.
[41] Padè HE. Sur la representation approchèe d'une fonction par des fractions rationnelles. Annales Scientifiques De l'École Normale Supérieure 1892;9:1–93.
[42] Leal HV, Guerrero F. Application of series method with padé and laplace-padé re-summation methods to solve a model for the evolution of smoking habit in spain. Computat Appl Mathem 2013;33(1):1–12.
[43] Rashidi MM, Keimanesh M. Using differential transform method and padé approximant for solving mhd flow in a laminar liquid film from a horizontal stretching surface. Math Probl Eng 2010;2010. Article ID 491319doi.org/10.1155/2010/491319.
[44] Guerrero F, Santonja F, Villanueva R. Solving a model for the evolution of smoking habit in spain with homotopy analysis method. Nonlinear Analysis: Real-World Application 2013;14(1):549–58.
[45] Wang Z, Zou L, Zong Z. Adomian decomposition and padé approximate for solving differential-difference equation. Appl Math Comput 2011;218(4):1371–8.
[46] Yang XS. Nature-Inspired metaheuristic algorithms. Luniver Press; 2008. ISBN 978-1-905986-10-1.
[47] Rao RV, Savsani VJ, Vakharia DP. Teaching–learning-based optimization: a novel method for constrained mechanical design optimization problems. Comput-Aided Des March 2011;43(3):303–15.
[48] Kennedy J, Eberhart R. Particle swarm optimization. In: IEEE international conference on neural networks; 1995. p. 1942–8.
[49] Storn R, Price K. Differential evolution—A simple and efficient heuristic for global optimization over continuous spaces. J Global Optim 1997;11:341–59.
[50] Goldberg DE. Genetic algorithms in search, optimization, and machine learning. Upper Saddle River: Pearson Education; 1989.
[51] Luqman M, Saeed M, Ali J, Tabassam MF, Mahmood T. Targeted showering optimization: training irrigation tools to solve crop planning problems. Pak J Agricult Sci 2019;56(1):225–35.
[52] Ali J, Saeed M, Tabassam MF, Iqbal S. Controlled showering optimization algorithm: an intelligent tool for decision making in global optimization. Comput Math Organ Theory 2019;25:132–64. https://doi.org/10.1007/s10588-019-09293-6.
[53] Eskandar H, Sadollah A, Bahreininejad A, Hamdi M. Water cycle algorithm – a novel metaheuristic optimization method for solving constrained engineering optimization problems. Comput Struct November 2012;110–111:151–66.
[54] Alatas B. Sports inspired computational intelligence algorithms for global optimization. Artif Intell Rev 2017. https://doi.org/10.1007/s10462-017-9587-x.
[55] Karaboga D, Basturk B. A powerful and efficient algorithm for numerical function optimization: artificial bee colony (ABC) algorithm. J Global Optim 2007;39:459–71.
[56] Mirjalili S, Mirjalili SM, Lewis A. Grey wolf optimizer. Adv Eng Software March 2014;69:46–61.
[57] Alexandros T, Georgios D. Nature-inspired optimization algorithms related to physical phenomena and laws of science: a survey. Intern J Artif Intell Tools 2017;26:750022.
[58] Wolpert DH, Macready WG. No free lunch theorems for optimization. IEEE Trans Evol Comput 1997;1(1):67–82.
[59] Price KV, Storn RM, Lampinen JA, editors. Differential evolution a practical approach to global optimization, natural computing series. Berlin: Springer; 2005. p. 479–98.
[60] Ali J, Saeed M, Chaudhry NA, Tabassum MF, Luqman M. Low cost-efficient remedial strategy for stagnated nelder-mead simplex method. Pak J Sci 2017;69(1):119–26.
[61] Nelder JA, Mead R. A simple method for function minimization. Comput J 1965;7(4):308–13.
[62] Mickens RE. A fundamental principle for constructing nonstandardnonstandard finite difference schemes for differential equations. J Differ Equations Appl 2005;11(7):645–53.